Supporting Information:

De-assembly of assembled Pt_1Ag_{12} units: tailoring the photoluminescence of atomically precise nanoclusters

Xi Kang,[‡,†] Lin Xiong,[‡,§] Shuxin Wang,[*,†] Yong Pei,[*,§] Manzhou Zhu[*,†]

[†]Department of Chemistry and Center for Atomic Engineering of Advanced Materials, Anhui Province Key Laboratory of Chemistry for Inorganic/Organic Hybrid Functionalized Materials, Anhui University, Hefei, Anhui 230601, China.
[§]Department of Chemistry, Key Laboratory of Environmentally Friendly Chemistry and Applications of MOE, Xiangtan University, Xiangtan, Hunan 411105, China.

Experimental Section

Materials

Hexachloroplatinic(IV) acid ($H_2PtCl_6\cdot6H_2O$, 99.99%, metal basis), silver nitrate ($AgNO_3$, 99%, metal basis), triphenylphosphine (PPh_3, 99%), sodium borohydride ($NaBH_4$, 99.9%), 2,4-dimethylbenzenethiol ($HSPhMe_2$, 99%), tetraphenylphosphonium bromide (PPh_4Br, 98%), bis-(diphenylphosphino)methane (dppm, $C_{25}H_{22}P_2$, 99%). Methylene chloride (CH_2Cl_2, HPLC grade, Aldrich), methanol (CH_3OH, HPLC, Aldrich). Pure water was purchased from Wahaha Co. Ltd. All reagents were used as received without further purification. All glassware were thoroughly cleaned with aqua regia (HCl: HNO_3 = 3:1 vol%), rinsed with copious pure water, and then dried in an oven prior to use.

Synthesis of $Pt_2Ag_{23}(PPh_3)_{10}Cl_7$ nanocluster

It should be noted that Bakr and coworkers have reported the synthetic method and crystal structure of $Pt_2Ag_{23}(PPh)_3Cl_7$ nanocluster,[1] and we now show an alternative synthetic method. For the $Pt_2Ag_{23}(PPh)_3Cl_7$ nanocluster synthesis, $AgNO_3$ (30 mg, 0.18 mmol) was dissolved in 5 mL CH_3OH, and $H_2PtCl_6\cdot6H_2O$ (3 mg, 0.006 mmol) was dissolved in 5 mL CH_3OH and added in. The solution was vigorously stirred (about 1200 rpm) with a magnetic stirring for 15 min. Then 265 mg (1 mmol) PPh_3 was dissolved in 30 mL CH_2Cl_2 and added in. After another 15 min, 1 mL $NaBH_4$ aqueous solution (20 mg/mL) was added quickly in the above mixture under vigorous stirring. The reaction was allowed to proceed for 24 hours under N_2 atmosphere. After reaction, the organic phase was evaporated under vacuum. Then, approximately 30 mL methanol was added to wash the synthesized products (for three times). The obtained precipitate was then dissolved into CH_2Cl_2 and evaporated, which produced $Pt_2Ag_{23}(PPh_3)_{10}Cl_7$ nanocluster (30 mg, 0.005 mmol, yield: 63% on the Ag mole basis).

Converting the $Pt_2Ag_{23}(PPh_3)_{10}Cl_7$ nanocluster into $[Pt_1Ag_{24}(SPhMe_2)_{18}](PPh_4)_2$ nanocluster

Typically, 10 mg $Pt_2Ag_{23}(PPh_3)_{10}Cl_7$ was dissolved in 10 mL of CH_2Cl_2. Then, 200 μL HS-$PhMe_2$ and 10 mg PPh_4Br were added to the solution simultaneously. The reaction was allowed to proceed for 30 min at room temperature. Then, the organic layer was evaporated to dryness. The $[Pt_1Ag_{24}(SPhMe_2)_{18}](PPh_4)_2$ nanocluster was obtained in this crude product. The dried nanocluster was washed with methanol at least 3 times and collected by centrifugation. The pure $[Pt_1Ag_{24}(SPhMe_2)_{18}](PPh_4)_2$ nanocluster was obtained by recrystallization process (1.5 mg, 0.0003 mmol, yield: 15% on the Ag mole basis).

Converting the $[Pt_1Ag_{24}(SPhMe_2)_{18}](PPh_4)_2$ nanocluster into $[Pt_1Ag_{12}(dppm)_5(SPhMe_2)_2]^{2+}$ nanocluster

Typically, 10 mg $[Pt_1Ag_{24}(SPhMe_2)_{18}](PPh_4)_2$ was dissolved in 10 mL CH_2Cl_2. Then, 30 mg dppm was added to the solution under vigorous stirring. The reaction was allowed to proceed for 15 min at room temperature. Then, the organic layer was evaporated to dryness. The $[Pt_1Ag_{12}(dppm)_5(SPhMe_2)_2]^{2+}$ nanocluster was obtained in this crude product. 20 mL of CH_3OH was used to extract the $[Pt_1Ag_{12}(dppm)_5(SPhMe_2)_2]^{2+}$ nanocluster, and the obtained solution was aged 24 hours in a freezer. Afterward, the yellow solution was centrifuged, and the supernatant was then evaporated to get the $[Pt_1Ag_{12}(dppm)_5(SPhMe_2)_2]^{2+}$ product (2.7 mg, 0.0007 mmol, yield: 23% on the Ag mole basis).

Characterization

All UV-vis absorption spectra of nanoclusters dissolved in CH_2Cl_2 were recorded using an Agilent 8453 diode array spectrometer, whose background correction was made using a CH_2Cl_2 blank. Solid samples were dissolved in CH_2Cl_2 to make a dilute solution firstly with a subsequent transformation to a 1 cm path length quartz cuvette, followed by spectral measurement.

Thermogravimetric analysis (TGA) was carried out on a thermogravimetric analyzer (DTG-60H, Shimadzu Instruments, Inc.) with 5 mg of nanocluster in a SiO_2 pan at a heating rate of 10 K min^{-1} from room temperature (about 298 K) to 1073 K.

X-ray photoelectron spectroscopy (XPS) measurement was performed on a Thermo ESCALAB 250, configured with a monochromated AlKα (1486.8 eV) 150 W X-ray source, 0.5 mm circular spot size, a flood gun to counter charging effects, and the analysis chamber base pressure lower than $1x10^{-9}$ mbar, data were collected with FAT=20 eV.

Photoluminescent (PL) spectra were measured on a FL-4500 spectrofluorometer with the same optical density (OD) ~0.05. In these experiments, the nanoclusters solution were prepared in CH_2Cl_2 at a concentration of less than 1 mg mL^{-1}.

Absolute quantum yields (QY) were measured with dilute solution of nanoclusters (0.05 OD absorption at 430 nm) on HORIBA FluoroMax-4P.

Inductively coupled plasma-atomic emission spectrometry (ICP-AES) measurements were performed on an Atomscan Advantage instrument made by Thormo Jarrell Ash Corporation (USA). The nanoclusters were digested by concentrated nitric acid and the concentration of the nanoclusters were set to 0.5 mg L^{-1} approximately.

Electrospray ionization time-of-flight mass spectrometry (ESI-TOF-MS) measurement was performed by MicrOTOF-QIII high-resolution mass spectromete.

DFT Calculations

The density functional theory (DFT) calculations were employed to optimize the geometric structure of nanoclusters using Perdew-Burke-Ernzerhof (PBE) functional[2] and the d-polarization included basis set (DND) was used for C, H, S, P elements. The DFT Semi-core Pseudopototential (DSPP) approximation with some degree of relativistic corrections into the core was used for the Ag and Pt elements implemented in the Dmol^3 package.[3,4]

Briefly, based on the Pt atom located at the center or the surface of M_{13}, more than 80 structural models of Pt_1Ag_{12} nanocluster are established according to the different bonding positions of the ligands on the surface. Then the relative energy of each isomer was obtained using the generalized gradient approximation with the Perdew-Burke-Ernzerhof (PBE) functional and the Double numerical (DND) basis set, implemented in the DMol^3 software package (in order to simplify the calculations, the phenyl and 2,4-dimethylphenyl are substituted with methyl).

References:

[1] Bootharaju, M. S.; Kozlov, S. M.; Cao, Z.; Harb, M.; Maity, N.; Shkurenko, A.; Parida, M. R.; Hedhili, M. N.; Eddaoudi, M.; Mohammed, O. F.; Bakr, O. M.; Cavallo, L.; Basset, J.-M. Doping-Induced Anisotropic Self-Assembly of Silver Icosahedra in $[Pt_2Ag_{23}Cl_7(PPh_3)_{10}]$ Nanoclusters. *J. Am. Chem. Soc.* **2017**, *139*, 1053-1056.

[2] Perdew, J. P.; Burke, K.; Ernzerhof, M. Generalized Gradient Approximation Made Simple. *Phys. Rev. Lett.* **1996**, *77*, 3865-3868.

[3] Delley, B. An All-Electron Numerical Method for Solving the Local Density Functional for Polyatomic Molecules. *J. Chem. Phys.* **1990**, *92*, 508-517.

[4] Delley, B. From molecules to solids with the DMol^3 approach. *J. Chem. Phys.* **2000**, *113*, 7756-7764.

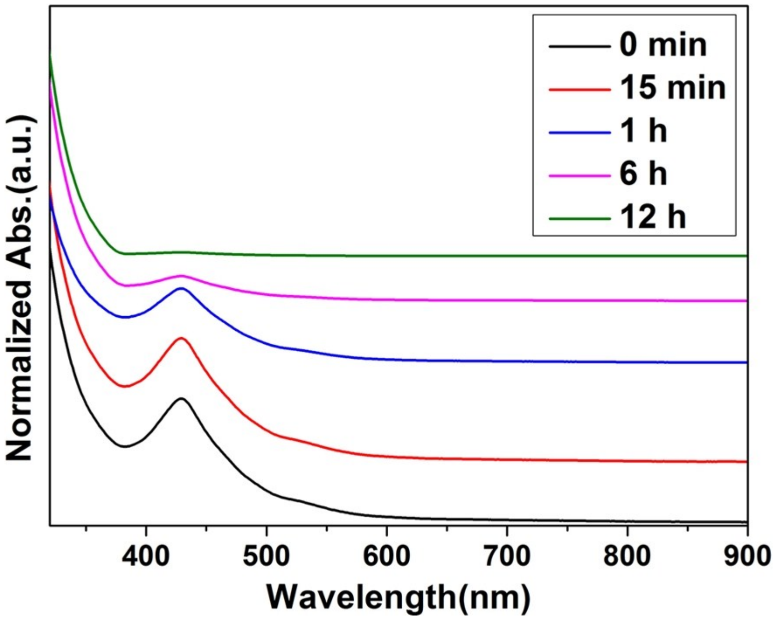

Fig. S1 UV-vis spectra confirming the thermal stability of $[Pt_1Ag_{12}(dppm)_5(SPhMe_2)_2]^{2+}$ nanocluster over time at room temperature (20 ^oC). Reaction condition: 10 mg $[Pt_1Ag_{12}(dppm)_5(SPhMe_2)_2]^{2+}$ dissolved in 10 mL CH_2Cl_2 underwent stirring with air.

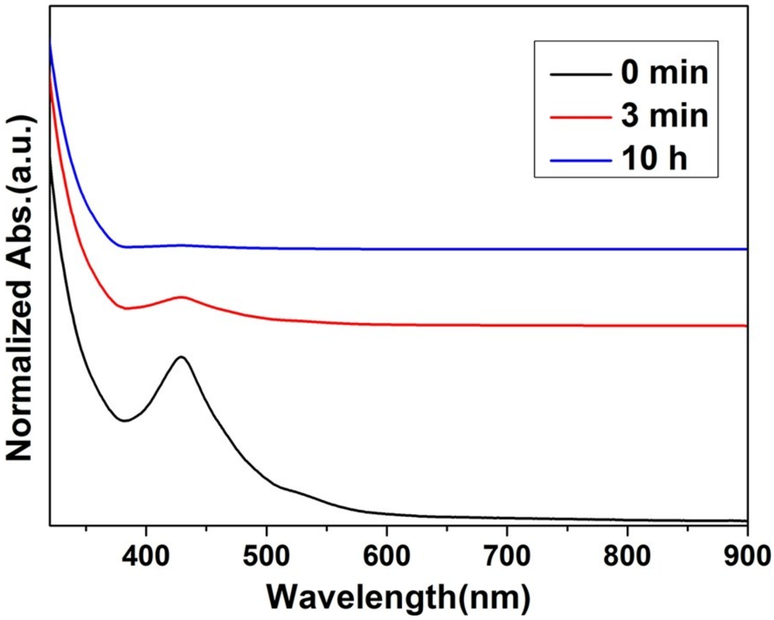

Fig. S2 UV-vis spectra confirming the thermal stability of $[Pt_1Ag_{12}(dppm)_5(SPhMe_2)_2]^{2+}$ nanocluster over time at 50 ^oC. Reaction condition: 10 mg $[Pt_1Ag_{12}(dppm)_5(SPhMe_2)_2]^{2+}$ dissolved in 10 mL CH_2Cl_2 underwent stirring with air.

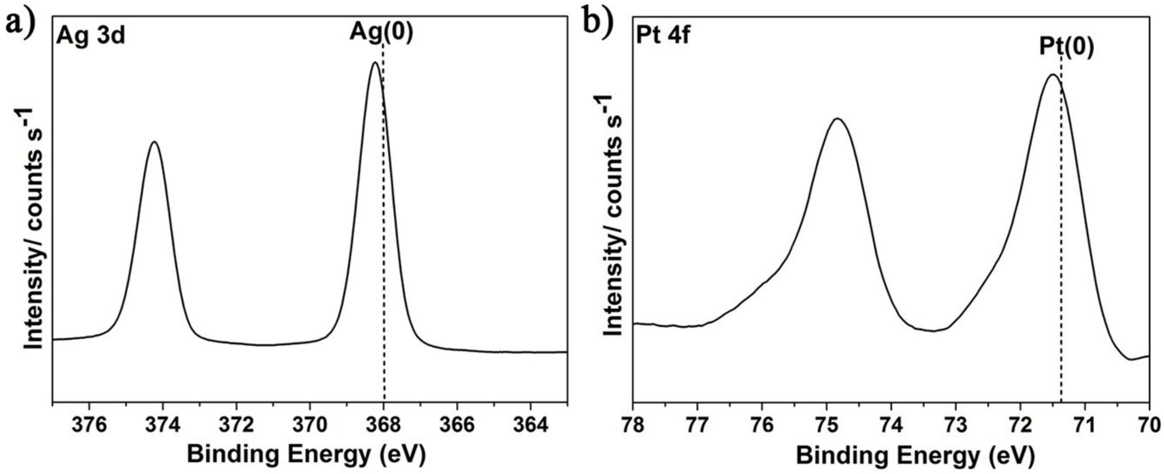

Fig. S3 X-ray photoelectron spectroscopy (XPS) of a) Ag 3d, b) Pt 4f in $[Pt_1Ag_{12}(dppm)_5(SPhMe_2)_2]^{2+}$ nanocluster.

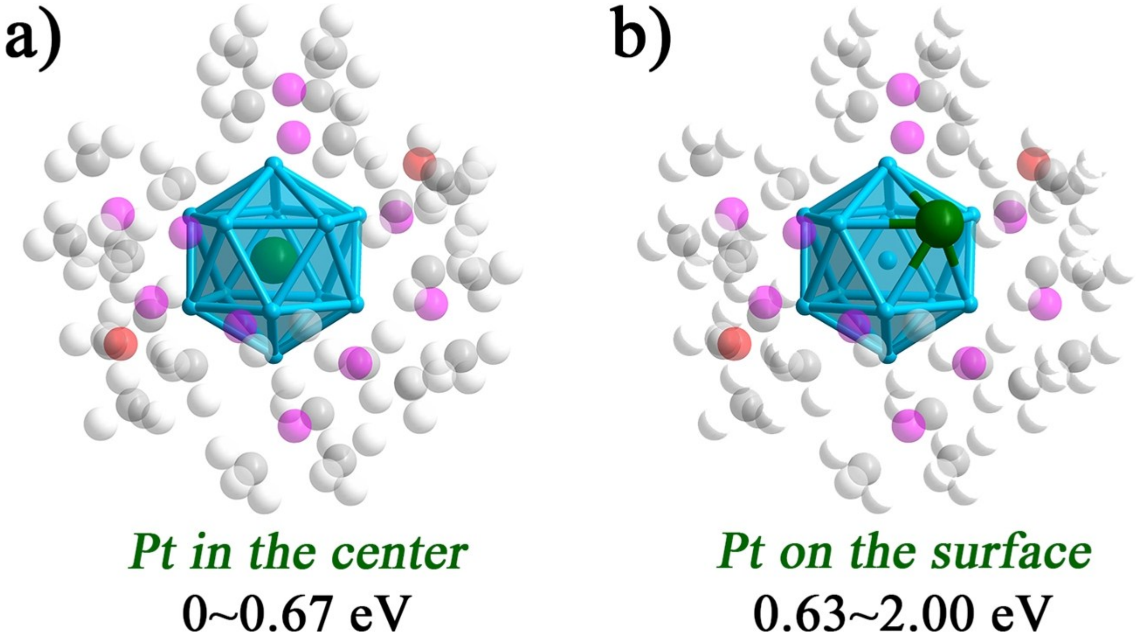

Fig. S4 The relative energy ranges of $[Pt_1Ag_{12}(dppm)_5(SPhMe_2)_2]^{2+}$ nanoclusters when the Pt atom was arranged a) in the central or b) on the surface of icosahedral M_{13} kernel. Color legend: dark green sphere, Pt; cerulean sphere, Ag; red sphere, S; purple sphere, P; grey sphere, C; white sphere, H.

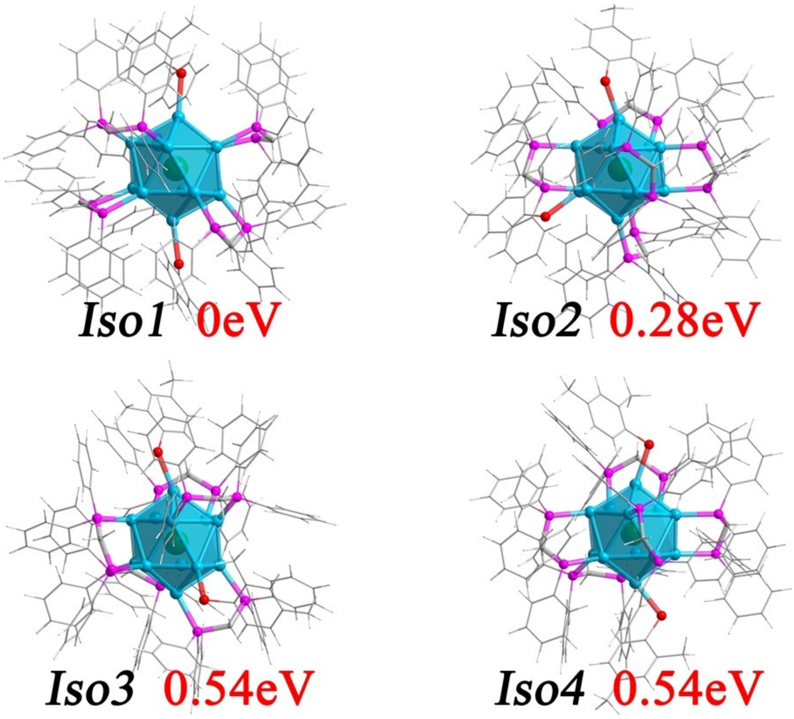

Fig. S5 The best four predicted isomers of Pt_1Ag_{12} nanocluster and the corresponding relative energies. Color legend: dark green sphere, Pt; cerulean sphere, Ag; red sphere, S; purple sphere, P; grey sphere, C; white sphere, H.

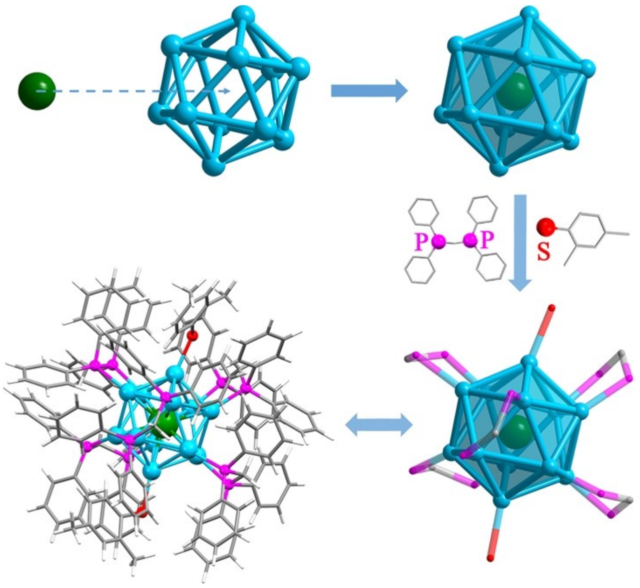

Fig. S6 The structural anatomy of $[Pt_1Ag_{12}(dppm)_5(SPhMe_2)_2]^{2+}$ nanocluster with lowest energy. Color legend: dark green sphere, Pt; cerulean sphere, Ag; red sphere, S; purple sphere, P; grey sphere, C; white sphere, H.

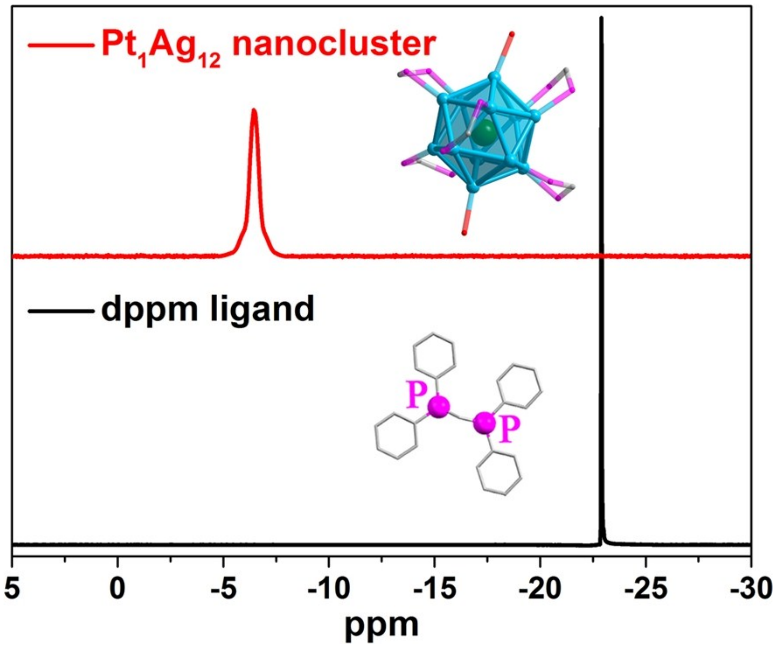

Fig. S7 The ^{31}P NMR results of dppm ligand and $[Pt_1Ag_{12}(dppm)_5(SPhMe_2)_2]^{2+}$ nanocluster. The result illustrates that all the phosphorous ends are in the almost same chemical environment, which further demonstrates that both phosphorous ends of diphosphine ligand connect with silver.

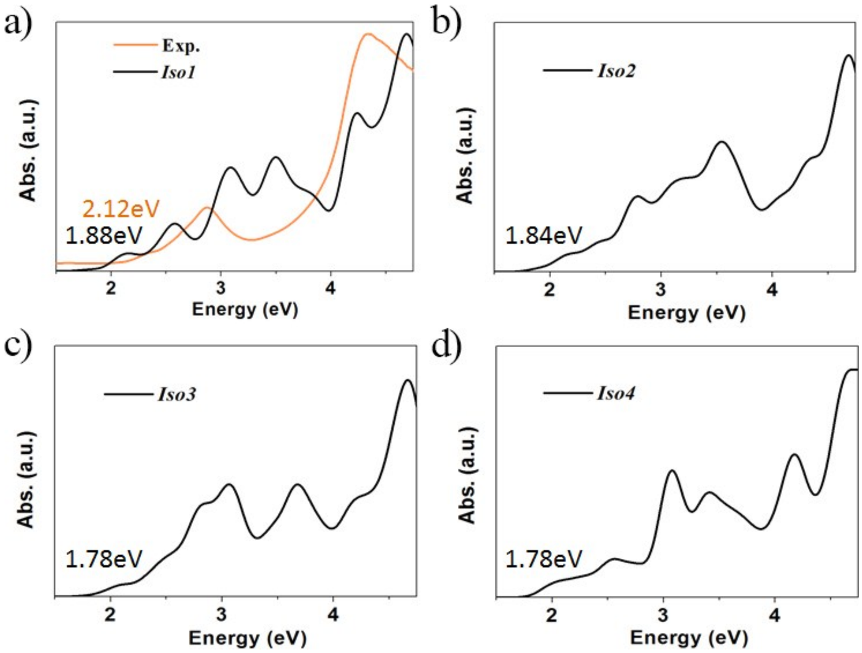

Fig. S8 The comparison of the optical absorption spectra of theoretically predicted structures (a for *Iso1*, b for *Iso2*, c for *Iso3*, d for *Iso4*, respectively) with the experimental optical absorption spectrum.

Photoluminescence is due to the electron transition from the valence band to the conduction band, and the excitation leads to the phenomenon of luminescence. In order to probe that whether the dramatic change in photoluminescence of mono-icosahedral $[Pt_1Ag_{12}(dmpm)_5(SMe_2)_2]^{2+}$ is caused by the change of ligand, we have calculated and compared the Kohn-Sham orbital diagrams and the HOMO-LUMO molecular orbitals of a mono-icosahedral $[Pt_1Ag_{12}(dmpm)_5(SMe_2)_2]^{2+}$ (**Di-P** nanocluster) and an assumed mono-icosahedral $[Pt_1Ag_{12}(tmp)_{10}(SMe_2)_2]^{2+}$ (**Mono-P** nanocluster), where two nanoclusters are different from the protection ligand as shown in Fig. S8. From Fig. S8, it is obviously that with the change of ligands, the energy levels and orbital composition of two nanoclusters are almost identical, which suggest that the change of the ligand layer has little influences on the electronic structure of metal cores and nanoclusters. Therefore, we propose that the ligand effect is not a major factor leading to significant changes in photoluminescence.

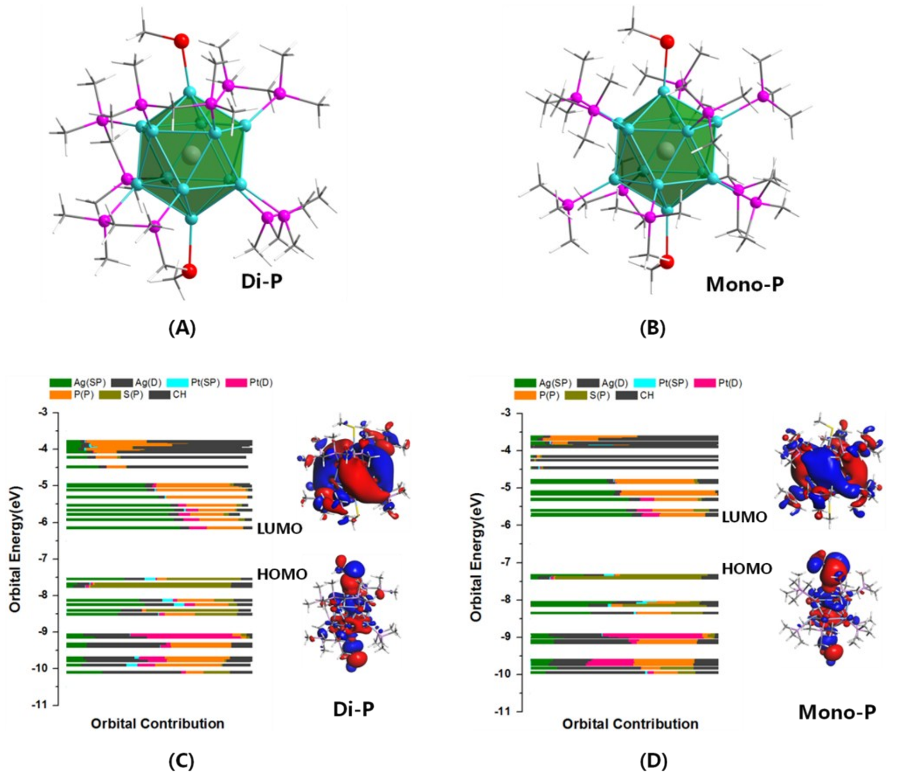

Fig. S9 Comparison of structure, Kohn-sham orbital energy levels and HOMO-LUMO molecular orbitals of two nanoclusters. Here, methyl is used to instead of R groups to simplify calculation. dmpm: 1,1-Bis(dimethylphosphino)methane; tmp: trimethyl-phosphine.

Table S1. The atomic ratio of Pt/Ag in Pt_1Ag_{12} nanocluster calculated by ICP and XPS measurements.

	Pt atom	Ag atom
ICP experimental ratio	7.47%	92.53%
XPS experimental ratio	7.38%	92.62%
Theoretical ratio	1/13(7.69%)	12/13(92.31%)